Electronic Supplementary Material (ESI) for Nanoscale.

Supporting Information

Confinement of Pt NPs by Hollow-Porous-Carbon-Sphere via Pore Regulation with Promoted Activity and Durability in Hydrogen Evolution Reaction

Zhuofan Gan,[a] Chengyong Shu,[a] Chengwei Deng,[b] Wei Du,[b] Bo Huang*[a] and Wei Tang*[a]

[a] *School of Chemical Engineering and Technology, Xi'an Jiaotong University, Xi'an 710049, P. R. China Email: bohuang@xjtu.edu.cn; tangw2018@xjtu.edu.cn*

[b] *State Key Laboratory of Space Power-Sources Technology, Shanghai Institute of Space Power Sources, Shanghai, 200245, P. R. China Email: dengchengwei@spacechina.com; sispdw@sina.com*

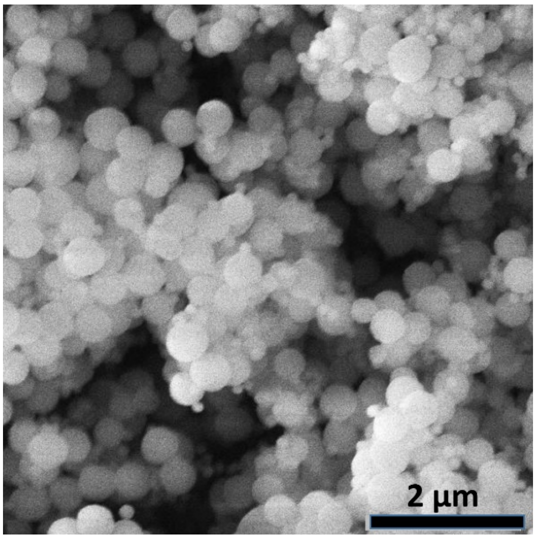

Fig. S1 The SEM image of silica spheres.

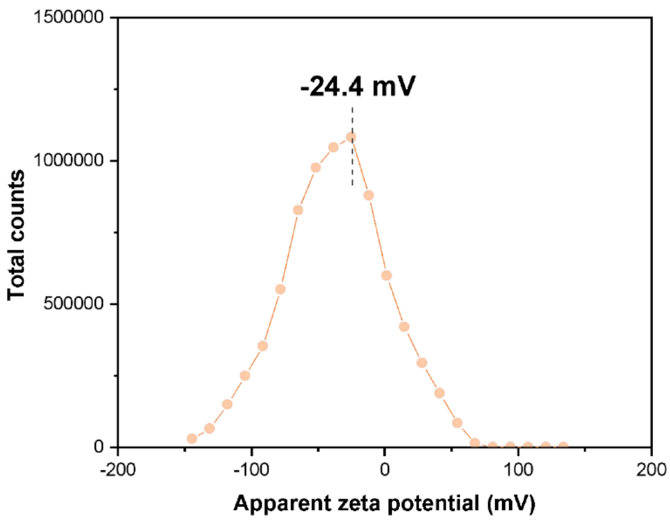

Fig. S2 Apparent zeta potential of the silica spheres in water / ethanol solution.

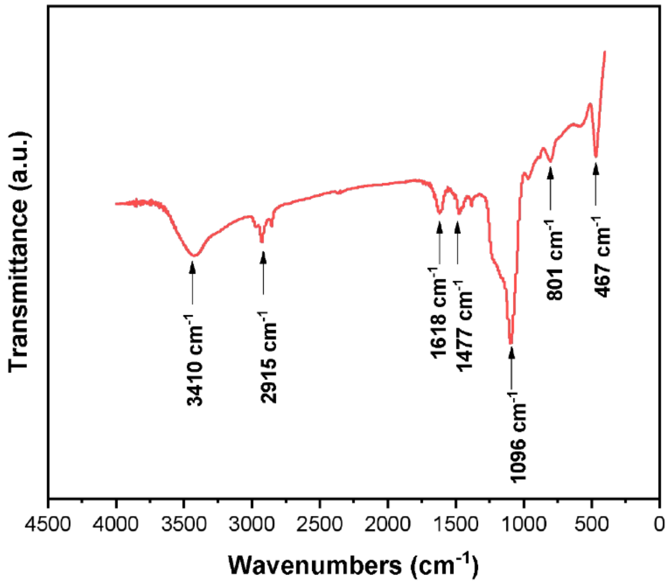

Fig. S3 FTIR spectra of the cross-link precursors.

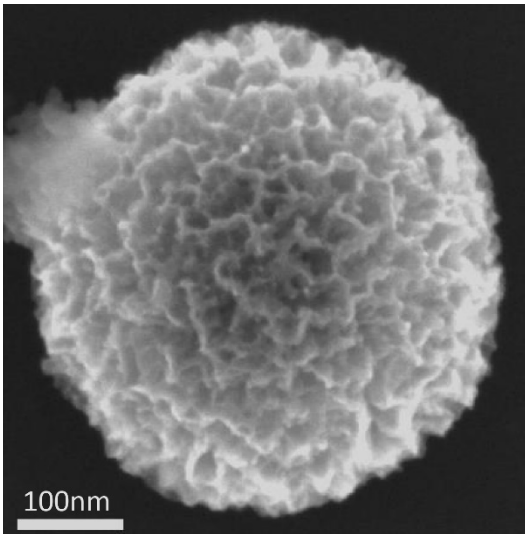

Fig. S4 The SEM image of N-HPCS obtained after 16 h of reaction.

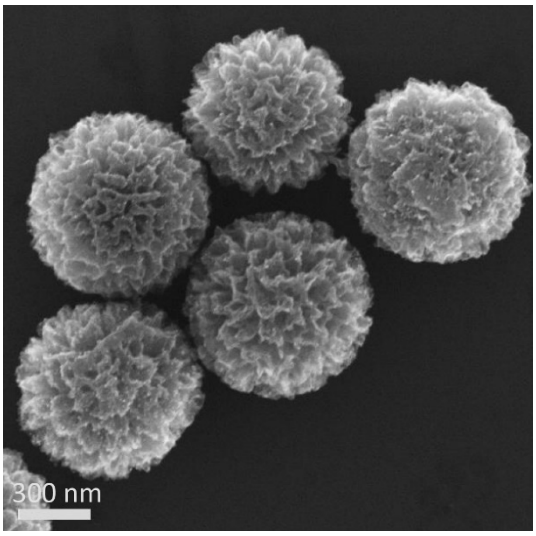

Fig. S5 The SEM image of N-HPCS-0.5.

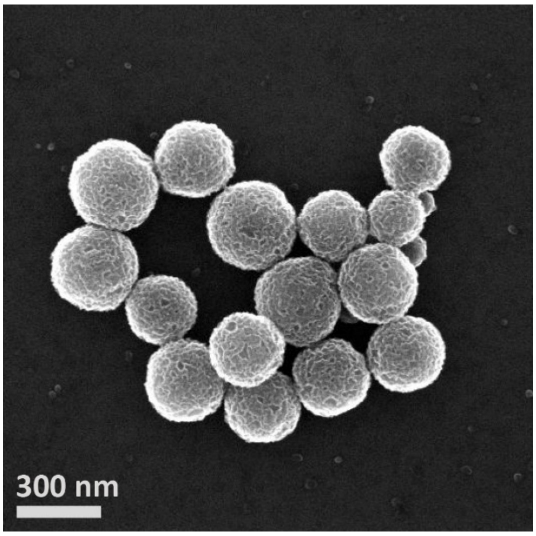

Fig. S6 The SEM image of N-HPCS-4.

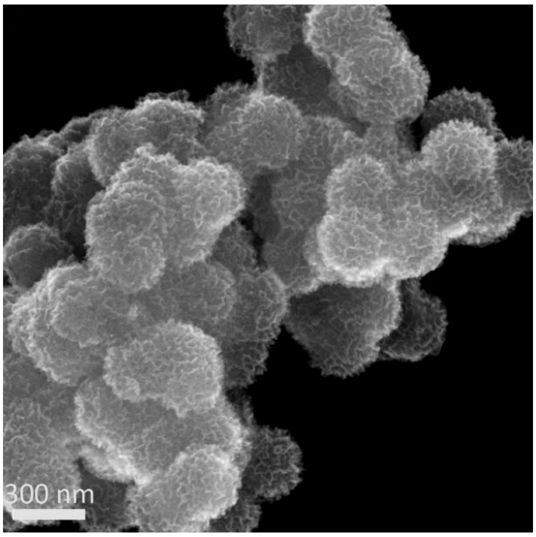

Fig. S7 The SEM image of N-HPCS-8

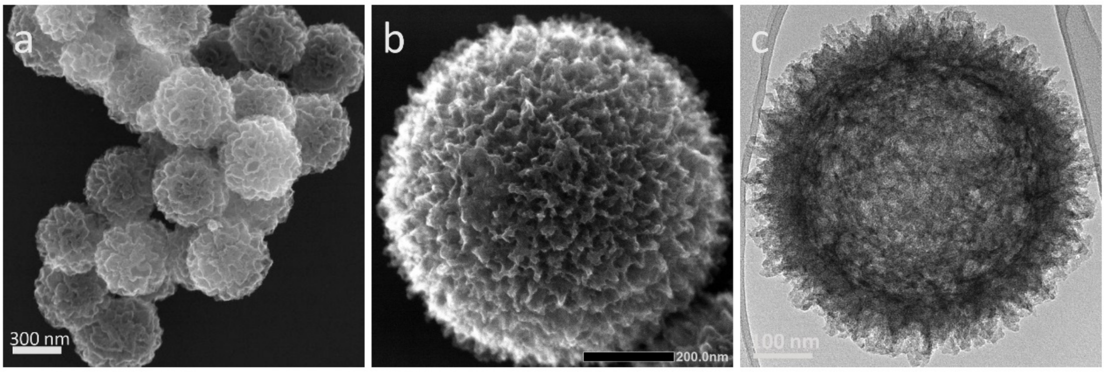

Fig. S8 The (a) SEM, (b) STEM and (c) TEM image of N-HPCS-2

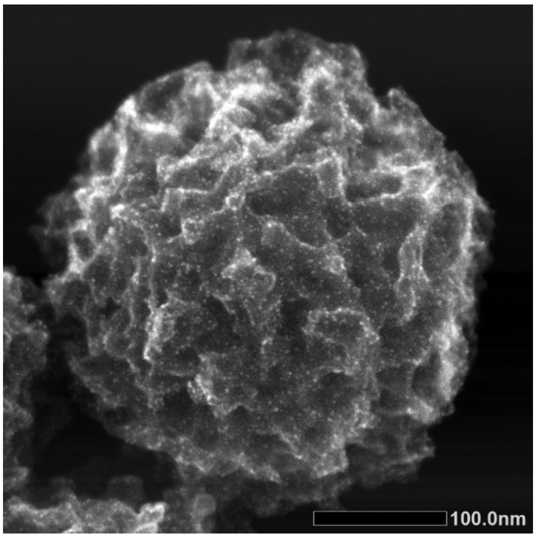

Fig. S9 The HAADF-STEM image of Pt/N-HPCS.

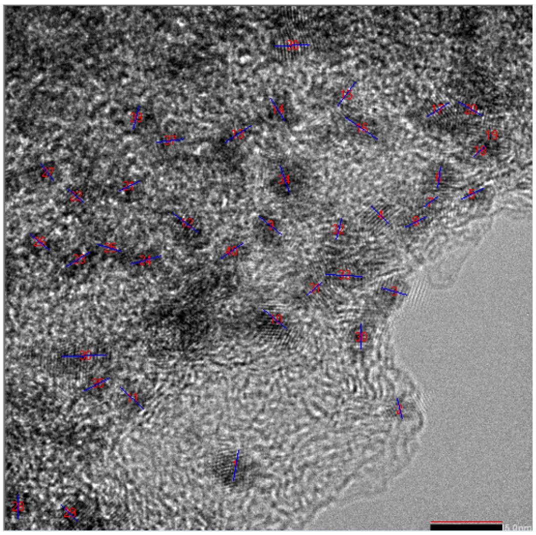

Fig. S10 Statistics of Pt NPs size on Pt/N-HPCS.

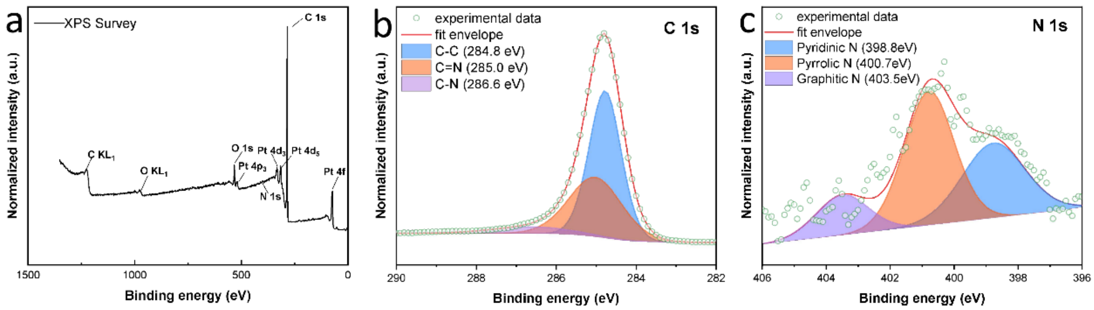

Fig. S11 (a) Surface survey XPS spectra of Pt(6.21%)/N-HPCS; (b) C 1s and (c) N 1s XPS spectra of Pt(6.21%)/N-HPCS.

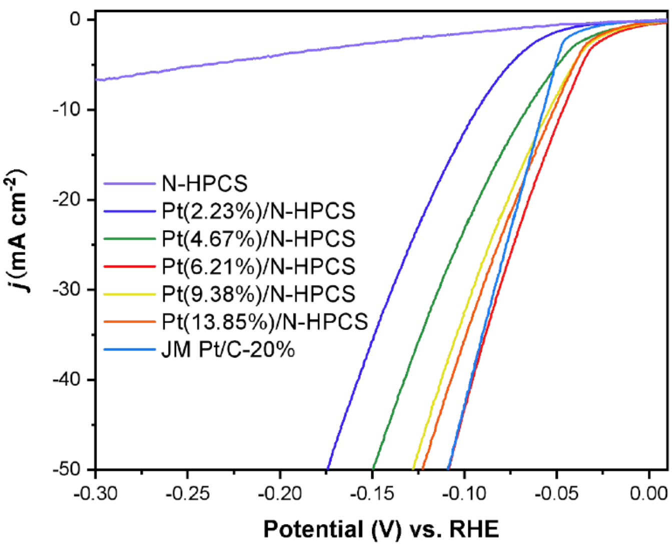

Fig. S12 LSV curves of N-HPCS, Pt/N-HPCS with different Pt loading amounts and JM Pt/C-20%.

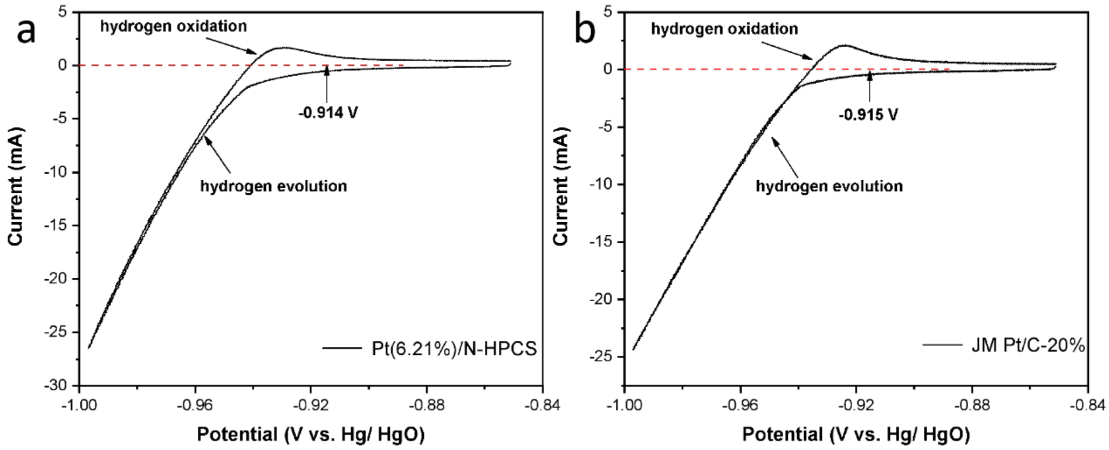

Fig. S13 The onset potentials of (a) Pt(6.21%)/N-HPCS and (b) JM Pt/C-20% in 1 M KOH solution. E(V, vs. RHE) = E(V, vs. Hg/ HgO) + 0.098 V + 0.0592 × 13.8. The solution was bubbled with hydrogen for 30min to get the H_2-saturated electrolyte before the test. Cyclic voltammetry (CV) was recorded at a scan rate of 2.0 mV s^{-1}. The average value of the two potentials corresponded to zero current was recognized as the onset potential of HER.

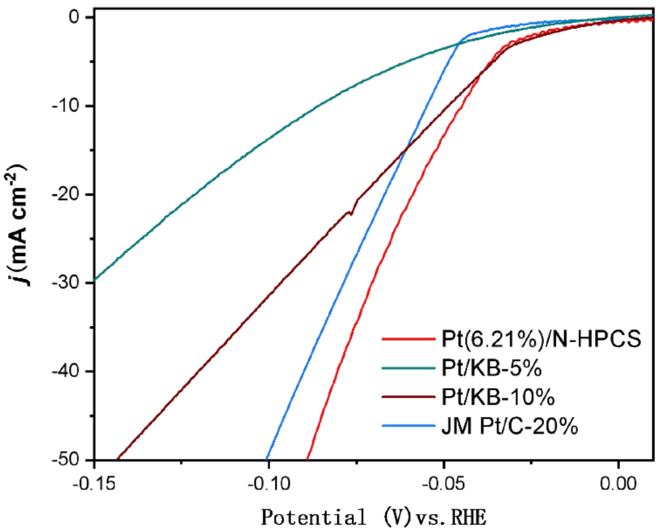

Fig. S14 LSV curves of Pt(6.21%)/N-HPCS, Pt/KB-5%, Pt/KB-10% and JM Pt/C-20% after iR-correction.

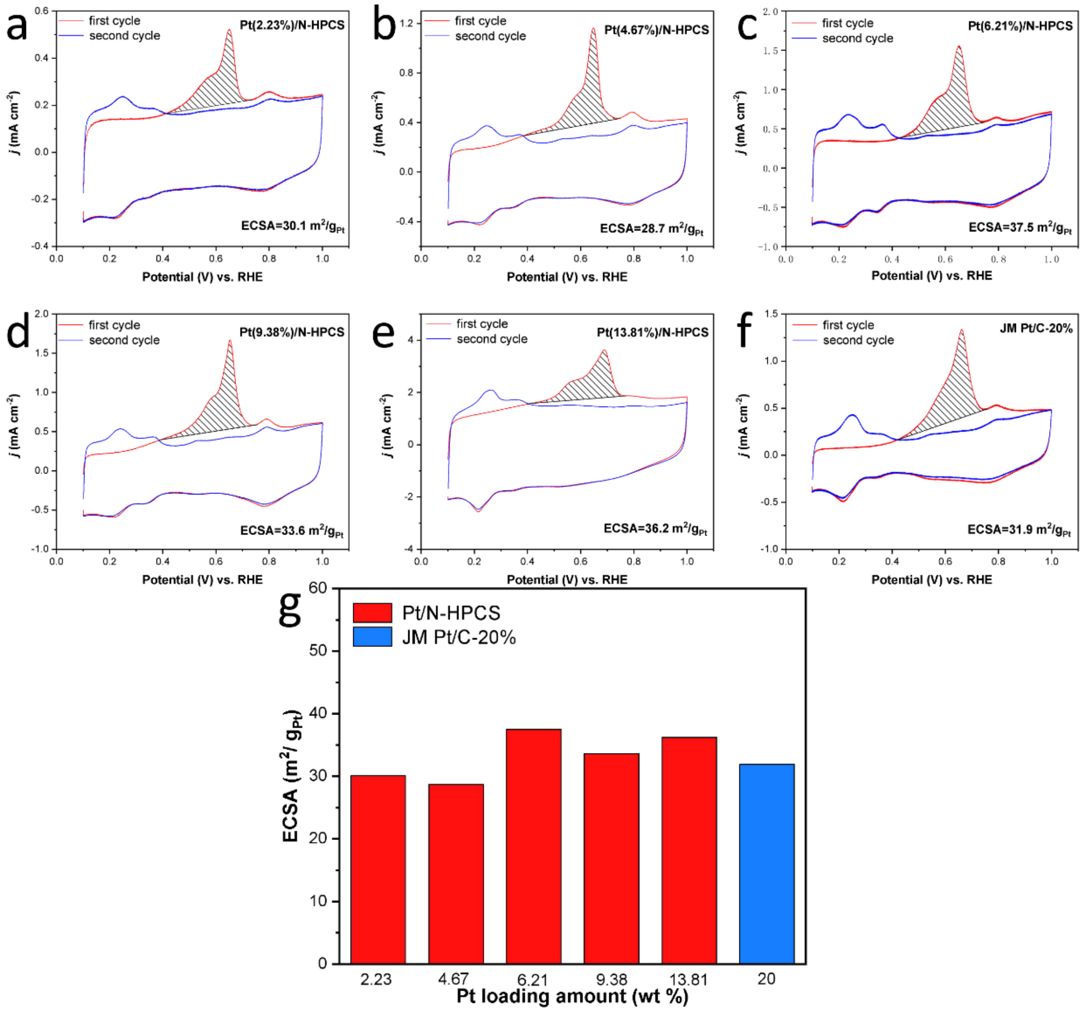

Fig. S15 CO stripping measurements of (a) Pt(2.23%)/N-HPCS, (b) Pt(4.67%)/N-HPCS, (c) Pt(6.21%)/N-HPCS, (d) Pt(9.38%)/N-HPCS, (e) Pt(13.81%)/N-HPCS and (f) JM Pt/C-20% in the solution of 1 M KOH at 20 mV s^{-1}. (g) The ECSAs of catalysts with different Pt loadings.

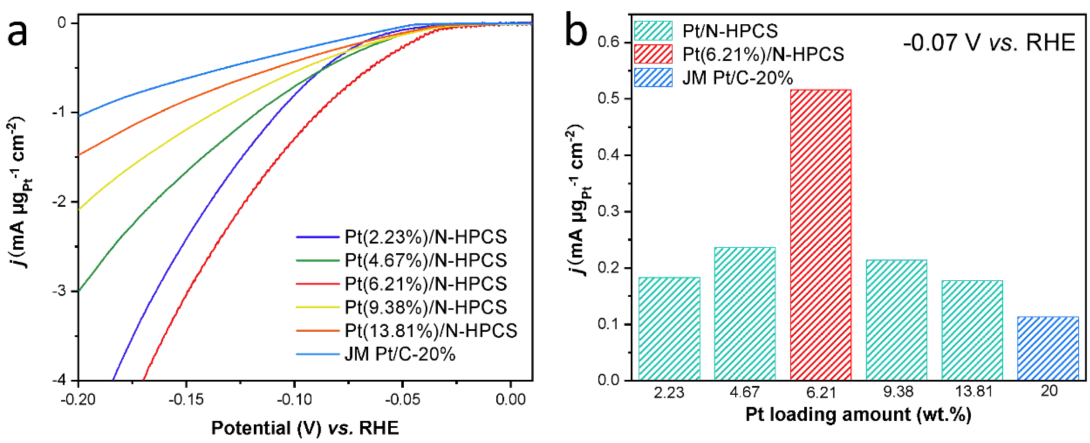

Fig. S16 (a) LSV curves of Pt/N-HPCS with different Pt loading amounts and JM Pt/C-20% based on the mass of Pt. (b) The mass activities of catalysts with different Pt loadings at -0.07 V (*vs.* RHE).

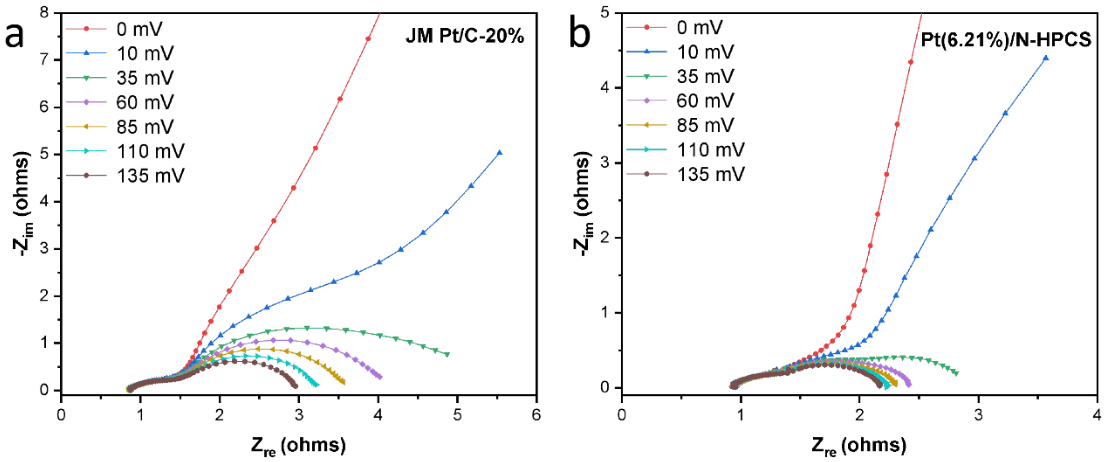

Fig. S17 Nyquist plots of (a) JM Pt/C-20% and (b) Pt(6.21%)/N-HPCS at various overpotentials. The EIS measurement was performed with a perturbation amplitude of 5 mV in the frequency range of 0.1 Hz to 100 kHz.

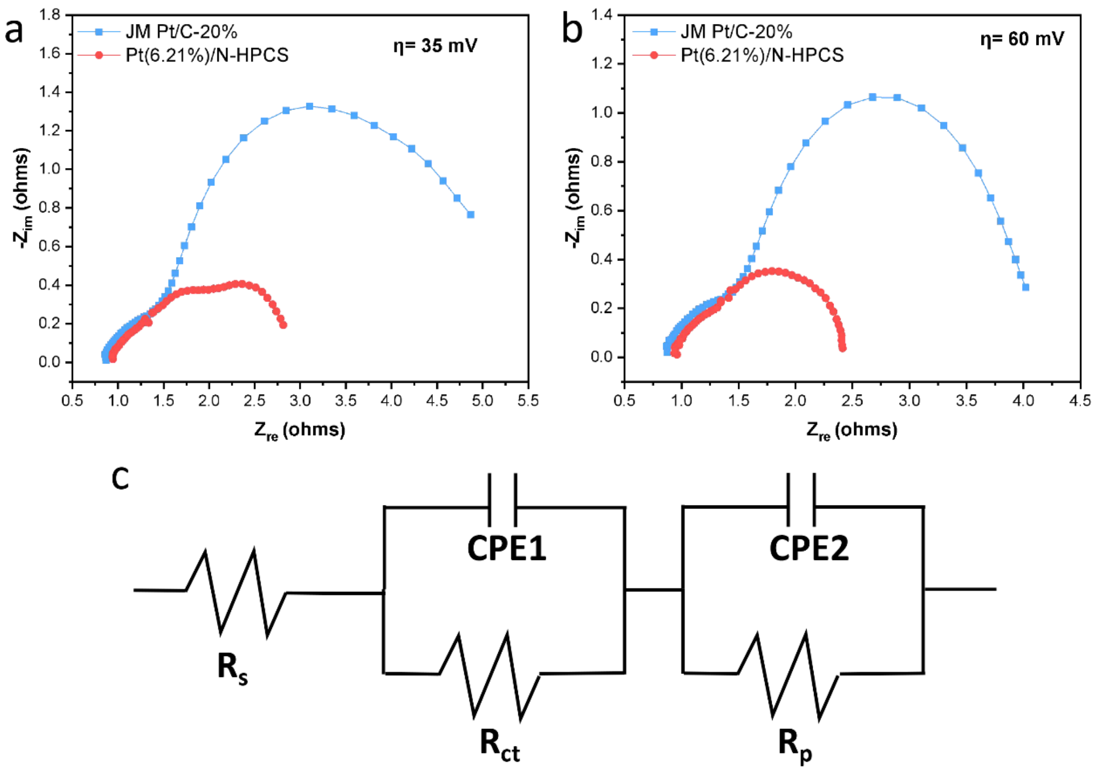

Fig. S18 Nyquist plots of JM Pt/C-20% and Pt(6.21%)/N-HPCS at overpotential of (a) 35 mV and (b) 60 mV. (c) The EIS data was simulated by equivalent electrical circuit diagram, containing of a series resistance (R_s), two constant phase components (CPE1 and CPE2), resistance related to surface porosity (R_p) and resistance related to charge transfer (R_{ct}). The EIS measurement was performed with a perturbation amplitude of 5 mV in the frequency range of 0.1 Hz to 100 kHz.

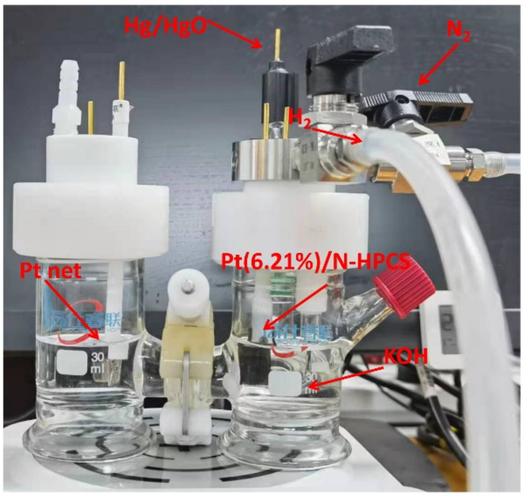

Fig. S19. The electrochemical cell for Faradaic efficiency measurement.

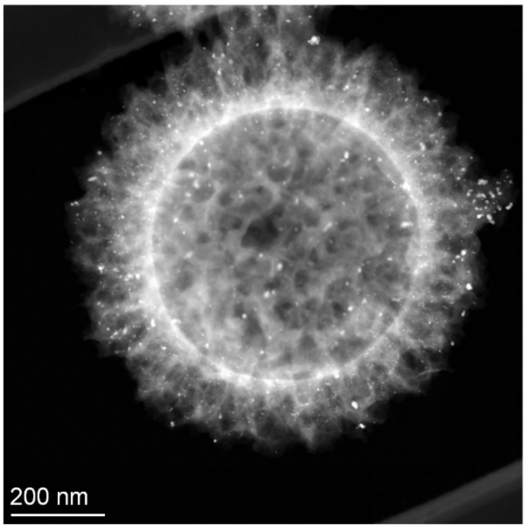

Fig. S20. The dark-field STEM image of Pt(6.21%)/N-HPCS after 60 h stability test.

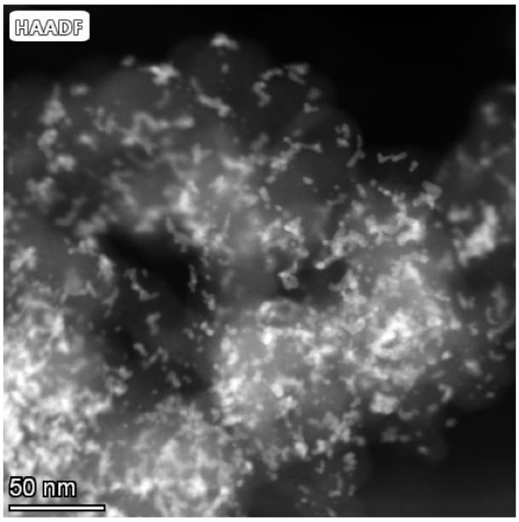

Fig. S21. The dark-field STEM image of JM Pt/C-20% after 20 h stability test.

Table S1 Elemental analysis of N-HPCS with different CTAB contents.

Sample	C (wt %)	H (wt %)	N (wt %)
N-HPCS-0.5	87.17	0.423	0.38
N-HPCS-1	72.97	1.793	1.52
N-HPCS-2	80.79	1.786	1.31
N-HPCS-4	72.75	2.377	1.08
N-HPCS-8	72.7	2.338	1.13

Table S2 BET specific surface areas of N-HPCS with different CTAB contents.

Sample	Dosage of CTAB (g)	BET surface area ($m^2 g^{-1}$)
N-HPCS-0.5	0.5	395.2
N-HPCS-1	1	740.9
N-HPCS-2	2	900.2
N-HPCS-4	4	638.2
N-HPCS-8	8	764.5

Table S3 ICP results of Pt contents in Pt/N-HPCS.

Sample	Pt contents (wt %)
Pt(2.23%)/N-HPCS	2.23
Pt(4.67%)/N-HPCS	4.67
Pt(6.21%)/N-HPCS	6.21
Pt(9.38%)/N-HPCS	9.38
Pt(13.81%)/N-HPCS	13.81

Table S4 Information about the electrochemical test in 1M KOH electrolyte.

Sample	Carbon paper	Catalyst loading (mg)	Pt loading (μg)	Overpotential at 10 mA/cm^2 (mV)
Pt(2.23%)/N-HPCS	1 cm × 1 cm	0.8	17.84	89.54
Pt(4.67%)/N-HPCS	1 cm × 1 cm	0.8	37.36	66.54
Pt(6.21%)/N-HPCS	1 cm × 1 cm	0.8	49.68	44.79
Pt(9.38%)/N-HPCS	1 cm × 1 cm	0.8	75.04	50.54
Pt(13.81%)/N-HPCS	1 cm × 1 cm	0.8	110.48	46.54
JM Pt/C-20%	1 cm × 1 cm	0.8	160.00	55.04
Pt/KB-5%	1 cm × 1 cm	0.8	40.00	86.25
Pt/KB-10%	1 cm × 1 cm	0.8	80.00	49.08

Table S5 Comparison of the HER performance of Pt NP catalysts in alkaline electrolyte.

Materials	Mass loading	Electrolyte	Overpotential at 10 mA/cm^2 (mV)	Tafel slope (mV/dec)	Ref.
Pt(6.21%)/N-HPCS	0.8 mg cm^{-2}	1 M KOH	45	22.4	this work
JM Pt/C-20%	0.8 mg cm^{-2}	1 M KOH	55	27.5	this work
Pt-NP/NiO-NS nanohybrids	0.1 mg cm^{-2}	1 M KOH with 1 M methanol	57	59.06	[1]
BC_3N@Pt	/	1 M KOH	26.1	41.59	[2]
Pt/$LiCoO_2$	0.204 mg cm^{-2}	1 M KOH	61	39.5	[3]
Pt@CoS_2-NrGO	3.0 mg cm^{-2}	1 M KOH	39	35	[4]
Pt/$Ni(HCO_3)_2$	/	1 M KOH	27	52	[5]
BP_{ed}-Pt/GR	14.28 μg_{Pt} cm^{-2}	1 M KOH	21	46.9	[6]
$Ni_{0.5}$-NCNFs-Pt	0.28 mg cm^{-2}	1 M KOH	47	31	[7]
3ZIF-67-Pt/RGO	20 μg_{Pt} cm^{-2}	1 M KOH	37.2	33.1	[8]
Pt-$Ni(OH)_2$-2h-NF20	20 μg_{Pt} cm^{-2}	1 M KOH	85	28	[9]

Table S6 TOF values of Pt(6.21%)/N-HPCS and JM Pt/C-20% in 1 M KOH.

Catalysts	Overpotential (mV vs. RHE)	TOF (H_2 s^{-1})
Pt(6.21%)/N-HPCS	100	1.263
	200	5.370
JM Pt/C-20%	100	0.310
	200	1.055

References

1 G. Ma, X. Zhang, G. Zhou and X. Wang, *Chem. Eng. J.*, 2021, **411**, 128292.
2 X. Zhao, M. Zheng, Z. Zhang, Y. Wang, Y. Zhou, X. Zhou and H. Zhang, *J. Mater. Chem. A*, 2021, DOI: 10.1039/d1ta04142h.
3 X. Zheng, P. Cui, Y. Qian, G. Zhao, X. Zheng, X. Xu, Z. Cheng, Y. Liu, S. X. Dou and W. Sun, *Angew. Chem., Int. Ed.*, 2020, **59**, 14533-14540.
4 N. Logeshwaran, S. Ramakrishnan, S. S. Chandrasekaran, M. Vinothkannan, A. R. Kim, S. Sengodan, D. B. Velusamy, P. Varadhan, J.-H. He and D. J. Yoo, *Appl. Catal., B*, 2021, **297**, 120405.
5 M. Lao, K. Rui, G. Zhao, P. Cui, X. Zheng, S. X. Dou and W. Sun, *Angew. Chem., Int. Ed.*, 2019, **58**, 5432-5437.
6 X. Wang, L. Bai, J. Lu, X. Zhang, D. Liu, H. Yang, J. Wang, P. K. Chu, S. Ramakrishna and X.-F. Yu, *Angew. Chem., Int. Ed.*, 2019, **58**, 19060-19066.
7 M. Li, Y. Zhu, N. Song, C. Wang and X. Lu, *J. Colloid Interface Sci.*, 2018, **514**, 199-207.

8 W. Wu, Z. Zhang, Z. Lei, X. Wang, Y. Tan, N. Cheng and X. Sun, *ACS Appl. Mater. Interfaces*, 2020, **12**, 10359-10368.
9 Q. Liu, Z. Yan, J. Gao, E. Wang and G. Sun, *ACS Appl. Mater. Interfaces*, 2020, **12**, 24683-24692.